

An impedance spectroscopy study of magnetodielectric coupling in BaTiO₃-CoFe₂O₄ nanostructured multiferroics

Ulises Acevedo, Rene Lopez-Noda, Romain Breitwieser, Francisco Calderon, Souad Ammar, and Raul Valenzuela

Citation: [AIP Advances](#) **7**, 055813 (2017); doi: 10.1063/1.4974493

View online: <http://dx.doi.org/10.1063/1.4974493>

View Table of Contents: <http://aip.scitation.org/toc/adv/7/5>

Published by the [American Institute of Physics](#)

Articles you may be interested in

[Nanopatterning spin-textures: A route to reconfigurable magnonics](#)

[AIP Advances](#) **7**, 055601055601 (2016); 10.1063/1.4973387

[Epitaxial growth of BiFeO₃ films on TiN under layers by sputtering deposition](#)

[AIP Advances](#) **7**, 055815055815 (2017); 10.1063/1.4974888

[Enhanced ferromagnetism in BiFeO₃ powders by rapid combustion of graphite powders](#)

[AIP Advances](#) **7**, 055803055803 (2016); 10.1063/1.4972806

[The magnetic properties of multiferroic BaCoF₄](#)

[AIP Advances](#) **7**, 055822055822 (2017); 10.1063/1.4976582

HAVE YOU HEARD?

Employers hiring scientists and engineers trust

PHYSICS TODAY | JOBS

www.physicstoday.org/jobs



An impedance spectroscopy study of magnetodielectric coupling in BaTiO₃-CoFe₂O₄ nanostructured multiferroics

Ulises Acevedo,^{1,2,a} Rene Lopez-Noda,³ Romain Breitwieser,²
Francisco Calderon,⁴ Souad Ammar,² and Raul Valenzuela^{1,2}

¹*Instituto de Investigaciones en Materiales, Universidad Nacional Autónoma de México, 04510, México*

²*ITODYS, Université Paris-Diderot, Sorbonne Paris Cité, CNRS-UMR 7086, 75205 Paris Cedex, France*

³*Departamento de Física Aplicada, Instituto de Cibernética, Matemáticas y Física, La Habana, Cuba*

⁴*Instituto de Ciencia y Tecnología de Materiales, Universidad de la Habana, La Habana, Cuba*

(Presented 2 November 2016; received 22 September 2016; accepted 28 October 2016; published online 17 January 2017)

Granular BaTiO₃-CoFe₂O₄ (BTO-CFO) nanocomposites were prepared by combining polyol synthesis and spark plasma sintering (SPS). This method allows samples with a high density and a very small grain size (less than 150 nm), and thus a large interface area between phases. In order to study the involved magnetoelectric effects, the impedance response of these nanomaterials was measured in the 5 Hz-10 MHz frequency range, under 0-7.5 kOe magnetic applied fields, and in the 40-170°C temperature range. The best agreement to model these results by an equivalent circuit was achieved by means of three parallel RC arrangements connected in series; by their RC values, these circuits are representative of grain boundaries. An association between each RC circuit and each interface (or grain boundary), *i. e.*, BTO-BTO, BTO-CFO, and CFO-CFO, is proposed on the basis of their temperature and magnetic behavior. © 2017 Author(s). All article content, except where otherwise noted, is licensed under a Creative Commons Attribution (CC BY) license (<http://creativecommons.org/licenses/by/4.0/>). [<http://dx.doi.org/10.1063/1.4974493>]

I. INTRODUCTION

Multiferroic materials can be defined as those materials exhibiting at least two ferroic orders, typically ferroelectricity and ferromagnetism, coupled in the same matrix.¹ The capability to interchange magnetic into electric energy and vice versa, makes these materials extremely useful in a large variety of potential applications in sensors, memories, actuators, microwave filters, read/lecture heads and other electronic devices.² Multiferroics are frequently classified in single phase, and multi-phase or composite multiferroics. The latter are currently attracting more attention since they present a stronger magnetoelectric (ME) effect at room temperature, and these effects can be extrinsic, as it is possible to tune them by varying the nature, the concentration and the shape of each phase.³ Multiferroics are typically characterized in terms of ME coupling coefficients.

Many models have been formulated for composite materials involving elastic interactions between different piezoelectric and magnetostrictive phases, giving rise to strain-mediated phenomena.⁴ However, interface charge-mediated mechanisms have been scarcely considered to understand ME coupling. These mechanisms recently appeared as playing an important role in composites with large contact area between strong correlated systems.⁵ Among extrinsic effects, a combination of magnetoresistance and the Maxwell-Wagner mechanisms has been discussed.⁶ In all the scenarios, nanoscaling could have a substantial impact on ME coupling.⁷

^aAuthor to whom correspondence should be addressed. Electronic mail: ulisesacsal@gmail.com.



To our knowledge, Impedance Spectroscopy techniques,^{8,9} based on measurements of the impedance of samples in a large frequency range and a deconvolution of the results to resolve the particular response of different parts of the sample (typically grains and grain boundaries), have seldom been used to investigate multiferroic materials. The Jonscher behavior was confirmed¹⁰ in PbZrTiO₃-NiZnFe₂O₄ nanocomposites prepared by a powder-in-sol precursor route, but no experiments under magnetic field were reported. In the case of BTO-LaSrMnO₃ system synthesized by sol-gel from nanopowders of the components, the dominant grain boundary effect in the response was observed,¹¹ but again, no frequency experiments under field were carried out. Frequency measurement in NiZn ferrites were presented,¹² but no deconvolution of results was carried out, just some analyses at fixed frequency were discussed (10 kHz).

In this manuscript, we present an Impedance Spectroscopy^{8,9} analysis of the ME response in BTO/CFO multiferroic nanocomposites obtained by a combination of *chimie douce* (polyol¹³) and Spark Plasma Sintering.¹⁴ This method allows to consolidate homogeneously mixed ferroelectric and ferrimagnetic nanoparticles (NPs) into a high density body (with densities above 95% of the theoretical density) at very low temperatures and extremely short times, retaining final sintered grain sizes at the nanoscale. Samples are measured in the 5 Hz-10 MHz frequency range in the 40-170°C and under magnetic fields in the 0-7.5 kOe. The usual techniques of Impedance Spectroscopy are used. When the impedance response of the several sections of the sample can be resolved, the estimated circuit elements can be associated with physical features of the material. This analysis allowed us to propose a correlation between the circuit elements and the BTO-BTO, CFO-CFO and BTO-CFO interfaces, and an interpretation of the ME obtained results.

II. EXPERIMENTAL PROCEDURES

BaTiO₃-CoFe₂O₄ nanocomposites were obtained by means of the SPS sintering technique starting from mixed (50-50%, molar) barium titanate (BTO) and cobalt ferrite (CFO) NPs, previously and separately synthesized by soft chemistry routes (forced hydrolysis in a polyol¹³). Structural, electrical and magnetic characterization, details on NPs synthesis and SPS procedures, as well as ME coupling evidences for the samples analyzed here can be found elsewhere.¹⁵ Disk sintered samples adapted with parallel gold electrodes over opposite faces (with a geometry factor d/A about 1000 m^{-1} , where d and A are the distance between electrodes and area of electrodes, respectively) were connected to an HP 4192 A impedance analyzer, placed in a small furnace and in an electromagnet (part of a 9600 LDJ VSM magnetometer). An AC electric signal was applied to the electrodes (1 V of amplitude) and a constant magnetic field was simultaneously applied to the sample. Before measuring, the sample was positioned in order to fix an angle of 90-degree between the electric and the magnetic fields (all data were obtained with this configuration). The AC electric field frequency was swept in 90 steps from 5 Hz to 10 MHz. Impedance measurements were carried out in the 40-170°C range under different magnetic fields (up to 7.5 kOe).

The SPS temperature profile for the consolidation of the CFO/BTO NPs mixture in the 1/1 ratio is shown in Fig. 1a. A 280°C-10 min plateau is used, in order to eliminate any organic remaining materials from the polyol reaction. The sintering was then carried out at 650°C for 5 min, after a 37°C/min heating rate. Finally, a rapid cooling rate was applied to avoid an additional grain growth. A SEM micrograph, shown in Fig. 1b, exhibited a microstructure constituted by grains in the 50-200 nm size range. BTO grains appeared a little smaller than CFO grains.

III. IMPEDANCE CHARACTERIZATION AND DISCUSSION

We first examined results obtained at $H = 0$ magnetic field. In the complex plane representation⁸ (also known as Cole-Cole plot), $Z'' = f(Z')$, where Z' and Z'' are the real and the imaginary part of impedance, respectively. The impedance response of samples was an arc, as shown in Fig. 2a. The size of these arcs decreased rapidly as temperature increased, as typically observed in many semiconducting oxides.¹⁶ In contrast with typical polycrystalline oxides, where this response can be modelled with two parallel RC circuits connected in series, in our case the best agreement was obtained with three parallel RC circuits, connected in series, with R_i and C_i equivalent elements

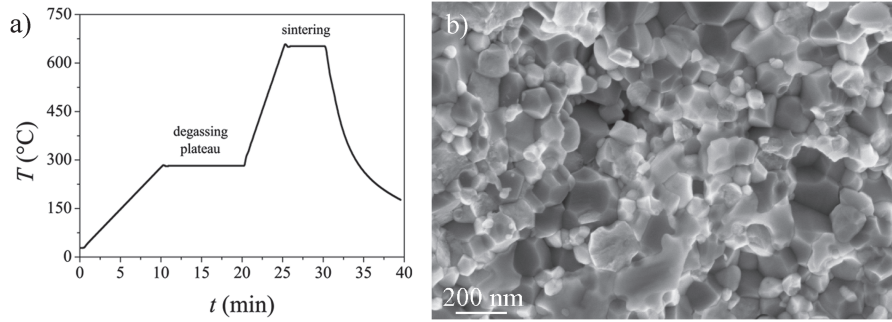


FIG. 1. a) Temperature profile followed in the SPS consolidation process, including a degassing step; b) SEM micrograph of the obtained microstructure.

in the $k\Omega$ and nF ranges, respectively. Since the estimated capacitance values correspond to grain boundary behavior,⁸ we can associate these impedance responses with the grain boundaries (or the interfaces) between the ferrite (CFO) and the titanate (BTO) phases: CFO-CFO, BTO-BTO and CFO-BTO. There was no evidence of additional components in the collected data, so the impedance responses of grains should have smaller relaxation times (given by $\tau = RC$ for each phase⁸), and are not apparent in the explored frequency range. Therefore, the produced materials can be broadly described as semiconducting grains with far more resistive grain boundaries. In order to search for a correspondence between the several RC arrangements and the different interfaces, an analysis of their behavior under different magnetic fields and temperatures were carried out.

The values of equivalent resistors, R_1 , R_2 and R_3 were quite different (Table I), but they exhibited the exponential decrease with T of a typical semiconductor. When plotted in an Arrhenius form, the activation energy can be extracted.¹⁶ Equivalent capacitances C_1 and C_3 exhibited the tendency of going through a maximum, Fig. 2b; capacitance C_2 , in contrast, exhibited a different thermal behavior, as it increased monotonically with T .

For this analysis, we chose to focus on the results obtained at a magnetic field of 7.5 kOe. At this field a high change in the magnetization of the ferrite was expected and its influence on the composite feature would be the most spectacular. For higher fields, the change in CFO magnetization is very small (the saturation is quite reached) while for smaller fields, the impedance response at all temperatures increases significantly (Fig. 3a for $T = 130^\circ\text{C}$). A new modelling of the response as a function of H led again to three parallel RC circuits in a series arrangement, with a clear increase in both R_i and C_i values. C_1 and C_3 showed again a wide maximum about 120°C , which in some way mimics the BTO transition from the ferroelectric to the paraelectric state. We can assume that these are representative of grain boundaries of BTO with itself, and BTO with CFO, as it has been found that grain boundaries in BTO contain a ferroelectric phase similar to ferroelectric grains.¹⁷ It

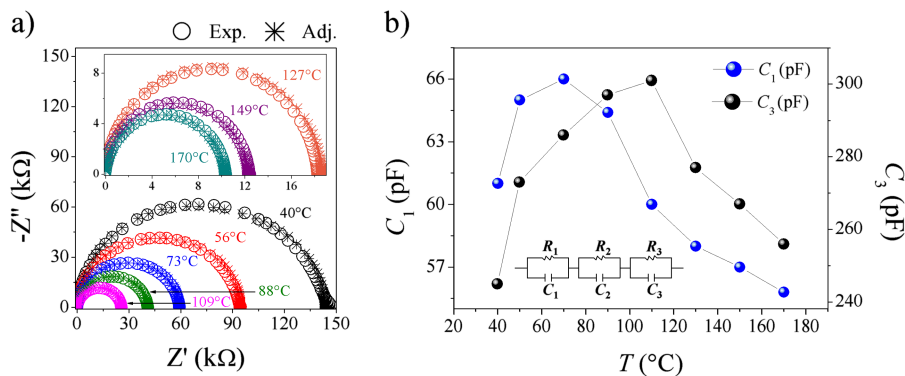


FIG. 2. a) Cole-Cole plots of impedance response at $H = 0$ and selected temperatures. In inset, the high temperature results with smaller impedance values; b) thermal behavior of C_1 and C_3 capacitance elements; in inset, the equivalent circuit modelled.

TABLE I. Estimated values of circuit elements.

T (°C)	R_1 (k Ω)		R_2 (k Ω)		R_3 (k Ω)		C_1 (pF)		C_2 (pF)		C_3 (pF)	
H (kOe)	0	7.5	0	7.5	0	7.5	0	7.5	0	7.5	0	7.5
40	91	256	51	210	2.3	6.5	61	111	307	530	245	502
50	53	182	40	160	1.4	5.1	65	124	274	532	273	539
70	34	108	24	128	0.99	4.23	66	167	265	586	286	625
90	25	68	15	70	0.79	2.51	64.4	173	293	719	297	593
110	18	52	7.3	45	0.63	2.56	60	176	393	926	301	489
130	14	30	4.1	24	0.52	3.33	58	204	548	1171	277	34
150	9.6	15	2.2	11	0.42	3.37	57	199	683	1288	267	27
170	8.2	9.5	1.6	7.6	0.37	3.47	55.8	218	816	1452	256	19.5

is difficult to distinguish between BTO-BTO and BTO-CFO, but based on estimated R and C values (Table I), it can be proposed that R_1C_1 represents BTO-CFO interfaces and R_3C_3 is associated with BTO-BTO boundaries, with larger values of capacitance. In contrast, C_2 exhibited again an increase with T , in some way antisymmetric to R_2 , as shown in Fig. 3b. In order to link the R_2C_2 to the CFO-CFO interfaces, an interpretation of the results on Fig. 3 should be proposed.

It is important to point out that in the present case, the sintering was performed under reductive operating conditions, namely, the starting nanopowders are compacted in a graphite crucible and maintained under vacuum during the whole axial pressure processing (see for instance^{15,18}). As a consequence, a partial reduction of Fe^{3+} into Fe^{2+} in the spinel phase occurs (less than 5 at %). Both cations prefer octahedral environments,¹⁹ and when they are on neighboring sites, a temperature $T \geq 120$ K provides enough energy for the Fe^{2+} extra electron to “hop” between Fe^{3+} - Fe^{2+} sites. The drop of several orders in magnitude of electric resistivity for magnetite ($\text{Fe}^{2+}\text{Fe}^{3+}_2\text{O}_4$) at this temperature is one of the signs of the Verwey²⁰ transition, reported in 1939. Therefore, this non-zero amount of Fe^{2+} is very probably high enough to induce a relatively high conductivity in the CFO grains. BTO is also sensitive to oxygen loss during sintering, which leads to an increase in conductivity.²¹ The presence of an inhomogeneous structure with strong differences in conductivity results in the creation of Schottky barriers, in which a concentration (or a depletion, depending on the applied electric field polarity) of carriers occurs, giving rise to a barrier layer capacitance.²² This phenomenon often explains the unusual high capacitance in polycrystalline oxides.²³ The presence of Fe^{3+} to Fe^{2+} pairs in octahedral sites leads, additionally, to the creation of electric dipoles in the ferrite phase,²⁴ contributing to the high values of capacitance. This is in good agreement with Fig. 3b, where estimated resistance and capacitance elements show an antisymmetric dependence with T .

In order to understand these results, the electric properties of ferrites should be revised. Anomalies in the magnetoresistance (MR) of ferrites, mainly MnFe_2O_4 , were first reported²⁵ in 1994. Not only

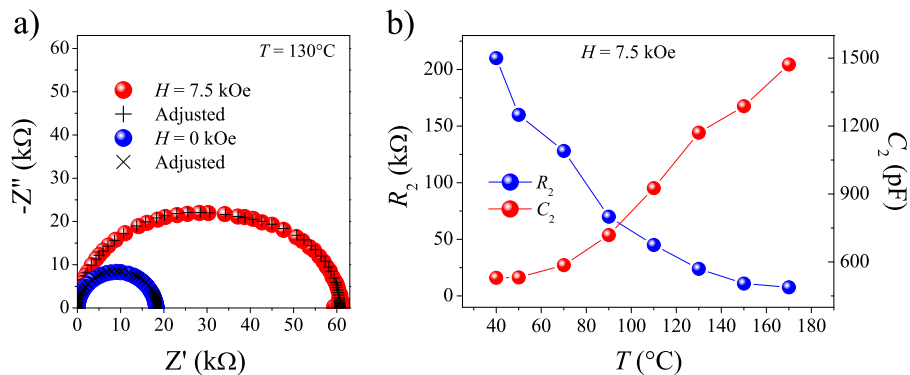


FIG. 3. a) Cole-Cole plot at $H = 0$ and 7.5 kOe, at 130°C ; b) thermal behavior of R_2C_2 components of the modelled equivalent circuit.

large values of negative MR were found, but strong differences between parallel and perpendicular MR measurements were observed. More recently, negative MR in ferrites has been reported²⁶ in CFO/CuO/CFO thin films prepared by magnetron sputtering, MnZn ferrites (with Fe₃O₄ and Ti⁴⁺ additives) produced²⁷ by solid state sintering, as well as in hexagonal, Z-type Sr₃Co₂Fe₂₄O₄₁ ferrites prepared by solid state sintering. In the case of CFO/SiO₂/p-Si thin film junction heterostructures²⁸ (synthesized by pulsed laser deposition), a negative MR was observed for the CFO film, whereas a positive MR was exhibited by the junctions.

In our case, according to the observed equivalent resistors R_i under magnetic field, a strong positive MR was observed on all the interfaces. This result can be explained if, as the reference reports, the nature of the interface can have an effect on the sign of MR. A factor which can be important is that our samples have been processed by a reductive method (SPS), as discussed before, leading to a larger amount of Fe²⁺ than typical solid state sintering techniques, normally carried out in air.

Our magnetocapacitance results can be thus explained in terms of a carrier-mediated effect. This coupling results entirely²⁹ from the selective accumulation of spin-polarized carriers at interfaces. Under the action of the electric field, free carriers are accumulated on grain boundaries. The observed behaviors of R_i and C_i with temperature and under magnetic field (Fig. 2b and Table I), indicate that carriers accumulated at BTO-CFO interfaces are also scattered by the magnetization of the ferrite. Under the effects of both the magnetization (CFO) and the polarization (BTO), the accumulation of spin-up carriers in the interfaces creates an imbalance, leaving behind an equivalent concentration of spin-down carriers. The overall result is the creation of an unusually high capacitance.

IV. CONCLUSIONS

An Impedance Spectroscopy (IS) analysis of ME effects in CFO/BTO nanocomposites in the 5 Hz-10 MHz frequency range, 40-170°C temperature range and 0-7.5 kOe magnetic field range, was presented. The IS methodology allowed the representation of the impedance response by means of three parallel RC circuits connected in series. Based on their elements values and their thermal behavior, an association of these circuits with the BTO-BTO, BTO-CFO and CFO-CFO interfaces was proposed. An interpretation of the strong increase in elements values upon the application of a magnetic field was proposed in terms of grain barrier layer capacitances and resistances, which are enhanced by the presence of Fe²⁺.

ACKNOWLEDGMENTS

U.A. thanks the National Science and Technology Council-Mexico (CONACyT) for a scholarship and R.V. acknowledges a sabbatical fellowship from DGAPA-UNAM (National Autonomous University of Mexico).

- ¹ D. N. Astrov, *Sov. Phys. JETP* **11**, 708 (1960).
- ² W. Eerenstein, N. D. Mathur, and J. F. Scott, *Nature* **442**, 759 (2006).
- ³ M. Fiebig and N. Spaldin, *Eur. Phys. J. B* **71**, 293 (2009).
- ⁴ V. M. Petrov, G. Srinivasan, M. I. Bichurin, and A. Gupta, *Phys. Rev. B* **75**, 224407 (2007).
- ⁵ T. Li, F. Zhang, K. Li, H. Wanga, and Z. Tang, *J. All. & Comp.* **638**, 344 (2015).
- ⁶ G. Catalan, *Appl. Phys. Lett.* **88**, 102902 (2006).
- ⁷ R. Ramesh and N. Spaldin, *Nature Mater.* **6**, 21 (2007).
- ⁸ J. T. S. Irvine, D. C. Sinclair, and A. R. West, *Adv. Mater.* **2**, 132 (1990).
- ⁹ J. R. Macdonald and E. Barsoukov, *Impedance Spectroscopy* (Wiley and Sons, Inc., Hoboken, New Jersey, 2005), p. 91.
- ¹⁰ D. K. Pradhan, R. N. P. Chowdhury, and T. K. Nath, *Appl. Nanosci.* **2**, 261 (2012).
- ¹¹ D. Nayek, P. Murugavel, D. Dinesh Kumar, and V. Subramanian, *Appl. Phys. A* **120**, 615 (2015).
- ¹² S. Banerjee, P. Hajra, A. Bhaumik, and D. Chakravorty, *Mater. Lett.* **79**, 65 (2012).
- ¹³ T. Gaudisson, M. Artus, U. Acevedo, F. Herbst, S. Nowak, R. Valenzuela, and S. Ammar, *J. Magn. Magn. Mater.* **370**, 87 (2014).
- ¹⁴ Z. A. Munir, U. Anselmi-Tanburini, and M. Ohyanagi, *J. Mater. Sci.* **41**, 763 (2006).
- ¹⁵ R. L. Noda, U. Acevedo, T. Gaudisson, F. Calderón Piñar, S. Ammar, and R. Valenzuela, *IEEE Trans. Magn.* **50**, 8002304 (2014).
- ¹⁶ D. C. Sinclair and A. R. West, *Phys. Rev. B* **39**, 13486 (1989).
- ¹⁷ N. Hirose and A. R. West, *J. Am. Ceram. Soc.* **79**, 1633 (1996).
- ¹⁸ R. Valenzuela, T. Gaudisson, and S. Ammar, *J. Magn. Magn. Mater.* **400**, 311 (2016).

- ¹⁹ R. Valenzuela, *Magnetic Ceramics* (Cambridge University Press, Cambridge, U. K., 2005), p. 8.
- ²⁰ E. J. W. Verwey, *Nature* **144**, 327 (1939).
- ²¹ F. D. Morrison, D. C. Sinclair, and A. R. West, *Int. J. Inorg. Mater.* **3**, 1205 (2001).
- ²² D. C. Sinclair, T. B. Adams, F. D. Morrison, and A. R. West, *Appl. Phys. Lett.* **80**, 2153 (2002).
- ²³ A. R. West, T. B. Adams, F. D. Morrison, and D. C. Sinclair, *J. Eur. Ceram. Soc.* **24**, 1439 (2004).
- ²⁴ D. I. Khomskii and J. Magn, *Magn Mater.* **306**, 1 (2006).
- ²⁵ K. P. Belov, *Phys. Uspekhi* **37**, 563 (1994). (Translation from *Uspekhi Fizicheskikh Nauk* **164**, 603(1994)).
- ²⁶ M. Djamal, R. Khairurrijal, and F. Haryanto, *Acta Phys. Pol. A* **128**, B-19 (2015).
- ²⁷ X. M. Xu and N. Zhang, *AIP Adv.* **5**, 117130 (2015).
- ²⁸ J. Panda and T. K. Nath, *Appl. Sci. A* **122**, 50 (2016).
- ²⁹ W. Eerenstein, N. D. Mathur, and J. F. Scott, *Nature* **442**, 759 (2006).